CORA Cork Open Research Archive Cartlann Taighde Oscailte Chorcaí

Title	A sustainable screen-printed Class-C rectifier for energy harvesting and wireless power transfer
Authors	Moloudian, Gholamhosein;Kumar, Sanjeev;Gawade, Dinesh R.;Buckley, John L.;O'Flynn, Brendan
Publication date	2025-05-21
Original Citation	Moloudian, G, Kumar, S, Gawade, D R, Buckley, J L & O'Flynn, B 2025, A sustainable screen-printed Class-C rectifier for energy harvesting and wireless power transfer. in 2025 19th European Conference on Antennas and Propagation (EuCAP). 19th European Conference on Antennas and Propagation, EuCAP 2025, Stockholm, Sweden, 30/03/25. https://doi.org/10.23919/EuCAP63536.2025.10999781
Type of publication	Conference item
Link to publisher's version	https://www.scopus.com/pages/publications/105007509216 - 10.23919/EuCAP63536.2025.10999781
Rights	© 2025, IEEE. Personal use of this material is permitted. Permission from IEEE must be obtained for all other uses, in any current or future media, including reprinting/republishing this material for advertising or promotional purposes, creating new collective works, for resale or redistribution to servers or lists, or reuse of any copyrighted component of this work in other works.
Download date	2026-09-19 17:57:43
Item downloaded from	https://hdl.handle.net/10468/18504

UCC
University College Cork, Ireland
Coláiste na hOllscoile Corcaigh

A Sustainable Screen-Printed Class-C Rectifier For Energy Harvesting and Wireless Power Transfer

Gholamhosein Moloudian*, Sanjeev Kumar, Dinesh R. Gawade, John L. Buckley and Brendan O'Flynn
Tyndall National Institute, University College Cork, Cork, T12R5CP, Ireland.
*Email: gh.moloudian@tyndall.ie

***Abstract*—This paper presents a novel, sustainable microwave Class-C rectifier for radio frequency (RF) energy harvesting and wireless power transmission. The proposed rectifier is fabricated using screen-printing techniques, utilizing a conductive layer made of silver nanoparticle ink and a sustainable cork substrate. The proposed rectifier consists of a simple matching network, a shunt diode, a Class-C harmonic termination structure and a resistive load. The proposed rectifier is designed to operate at f = 2.4 GHz, achieving a peak power conversion efficiency (PCE) of 64% at an RF input power (P_{IN}) level of 24 dBm and an optimal load (R_{L}) of 160 Ω. In the latter case, a DC-DC boost converter and a supercapacitor (C_{OUT} = 0.33 F) are employed to ensure adequate DC voltage for powering Internet of Things (IoT) devices, validating the rectifier's performance. The proposed system successfully demonstrates the charging of both the DC-DC booster and the supercapacitor across different P_{IN} levels. Notably, this is the first time that a Cork substrate has been utilized for designing a microwave Class-C rectifier circuit, highlighting its potential for future sustainable IoT applications and RF circuitry design.**

***Index Terms*—Class-C Rectifier, Energy Harvesting, Screen-printed, Sustainable Cork Substrate, Wireless Power Transfer (WPT).**

I. Introduction

In recent years, interest in energy harvesting and wireless power transmission (WPT) has significantly increased, with the objective of developing battery-free sensing systems and self-sustaining Internet of Things (IoT) devices [1]–[4]. Moreover, recently, there has been an increasing focus on employing sustainable, biodegradable materials combined with additive manufacturing technologies to develop eco-friendly RF circuits for next-generation wireless communications, particularly for sustainable IoT applications [5], [6]. Technological advancements in RF circuits have relied heavily on substrates like FR4 and Rogers, which provide excellent high-frequency performance. However, these conventional materials are not considered to be sustainable and can significantly contaminate the environment if not disposed of correctly, highlighting the need for more natural sustainable and eco-friendly alternatives [7].

Cork, a natural biodegradable material, is attracting significant attention as a potential key component in the future of sustainable RF circuits, particularly for sensor and antenna design [8], [9]. Its capacity to minimize the environmental impact of electronic devices makes it a compelling alternative to standard non-sustainable materials. Beyond its eco-friendly attributes, cork is also cost-effective, lightweight, and flexible,

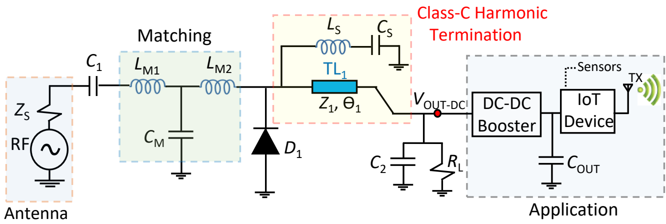

Fig. 1. Proposed topology for powering IoT sensing devices.

offering sustainability in conjunction with a low dielectric constant. These qualities make it a good choice for developing RF circuits, and especially antennas and sensors, supporting the movement towards greener and more sustainable electronics [8]–[14]. Current literature primarily focuses on the use of cork materials for designing and developing antennas and sensors, with no reports on their application in RF circuit design. Therefore, considering cork for RF circuits is a novel approach in developing environmentally friendly devices, and its promising characteristics in this regards make it a strong candidate for achieving sustainability goals.

Energy harvesting and wireless power transfer are promising techniques for supplying sufficient direct current (DC) power to power the next generation of low-power electronic circuits and IoT devices [1], [2], [4]. At the core of these systems are rectifying-antennas (rectennas) [15], which play a crucial role in capturing RF signals and converting them into DC power. A rectenna circuit consists of an antenna and a rectifier circuit. The antenna serves as a fundamental component in rectenna circuits, tasked with harvesting and transferring RF signals [3], [16]. Similarly, the rectifier is essential for energy harvesting and wireless power transfer, as it converts the captured RF signals into DC power. However, rectifiers are non-linear electronic circuits that produce several high-order unwanted harmonics during the rectification process [17], [18]. These harmonics cause power dissipation in the diode rectifiers, negatively affecting the RF-to-DC power conversion efficiency (PCE). Controlling these harmonics is essential to enhance PCE and increase the DC output voltage ($V_{\mathrm{OUT-DC}}$) [17], [18].

In recent years, various techniques have been implemented to control harmonics, including low-pass filter (LPF) structures [17]–[26], harmonic termination methods in Class-F [27]–[29], Class-F^{-1} [30]–[32], and Class-C configurations [33], as well as harmonic recycling approaches [34]. These methods effectively manipulate the current and voltage waveforms of

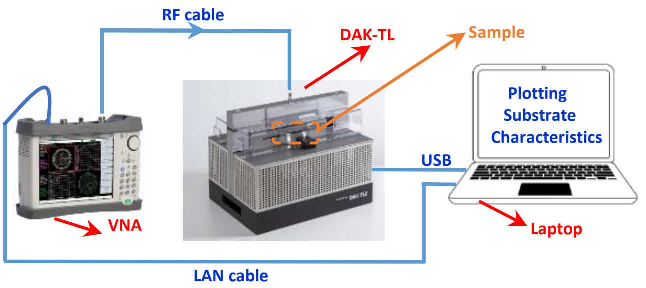

Fig. 2. DAK-TL system setup for dielectric measurements of the sustainable Cork sustrate. Equipment: DAK-TL: dielectric assessment kit (DAK3.5-TL) from Speag [35], VNA: Anritsu MS2038C, Sample: Cork substrate.

the rectifier diodes to minimize their overlap, thereby reducing power consumption in the diodes. However, the current state of the art indicates that most designed rectifier circuits rely on non-sustainable materials, typically high-frequency substrates such as FR4 and Rogers materials [17]–[34].

This paper presents a novel microwave rectifier that, for the first time, utilizes screen-printing technology on a sustainable Cork substrate for RF energy harvesting and WPT applications. Fig. 1 illustrates the proposed rectifier, designed for charging a DC-DC booster, a supercapcitor (C_{OUT} = 0.33 F) and powering IoT sensing devices. To succinctly summarize the main contributions, the key innovations of this research can be outlined as follows:

- Rectifier Design Methodology: The proposed rectifier utilizes an innovative class-C harmonic termination structure designed to allow the passage of the DC frequency signal while controlling harmonics up to the fourth order. This harmonic termination structure reshapes the current and voltage waveforms of the Schottky diode to minimize their overlap, effectively reducing power loss in the diode. As a result, this approach enhances the DC voltage signal, leading to improved PCE and overall rectifier performance. Moreover, to validate the rectifier performance, a DC-DC booster and a supercapacitor was powered for varying P_{IN} levels.
- Manufacturing Process: For the first time in the field, the proposed Class-C rectifier is designed on a sustainable cork substrate. Additionally, the manufacturing process utilizes a screen-printing technique combined with nanometer-scale silver ink. This approach creates new opportunities for designing RF circuits with a focus on sustainability.

The rest of the paper is structured as follows: Section II covers the design aspects of the proposed Class-C harmonic termination network and the manufacturing process of the proposed rectifier. Section III provides an in-depth analysis of the rectifier's performance in powering an electronic load. Finally, Section IV outlines the main conclusions of this study.

II. Rectifier Design Methodology

To design the proposed circuit, the initial step involves determining the permittivities of the Cork substrate. As depicted in Fig. 2, for this purpose, the DAK-TL system is utilized

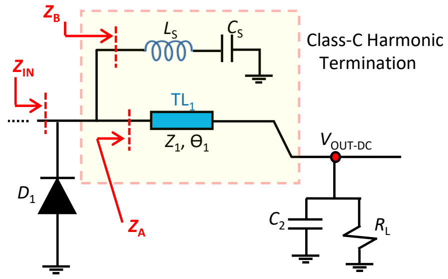

Fig. 3. Schematic of the proposed Class-C harmonic termination structure.

to measure key parameters such as the dielectric constant (ϵr), loss tan(δ), and additional substrate properties across a range of frequencies. The rectifier is implemented on a cork substrate, chosen for its sustainability, featuring a relative permittivity of ϵ_r = 1.39 and a loss tangent of $tan\delta$ = 0.038 at 2.4 GHz. These dielectric characteristics were determined using a dielectric assessment kit (DAK3.5-TL) from Speag [35]. For the simulation and design process, the conductive layer was modeled as a metallic layer with a thickness of 10μm and a conductivity of 3.94×10^6 S/m at 2.4 GHz. In the following, an in-depth discussion of the Class-C harmonic termination structure and the rectifier design will be presented in subsections A and B, respectively.

A. Class-C Harmonic Termination Design Theory

In this paper, the proposed rectifier circuit incorporates an innovative Class-C harmonic termination network to control rectifier harmonics across multiple frequencies (f = DC, f_0, $2f_0$, $3f_0$ and $4f_0$). The proposed Class-C harmonic network is designed and simulated using the commercial software, Keysight Advanced Design System (ADS). Fig. 3 depicts the proposed class-C harmonic network, which consists of a series filter and a transmission line (TL_1 = λ/4, a quarter wavelength line), in parallel. According to design theory, the impedance termination for the proposed Class-C network can be expressed as

$$Z_{\mathrm{A}} = \begin{cases} R_L & \omega = 0 \\ \infty & \omega = \omega_0, 3\omega_0, \ldots \\ 0 & \omega = 2\omega_0, 4\omega_0, \ldots \end{cases} \quad (1)$$

$$Z_{\mathrm{X}} = \begin{cases} \infty & \omega = 0 \\ j\omega_0 L_s + \frac{1}{j\omega_0 C_s} & \omega = \omega_0 \\ j2\omega_0 L_s + \frac{1}{j2\omega_0 C_s} & \omega = 2\omega_0 \\ 0 & \omega = 3\omega_0 \end{cases} \quad (2)$$

$$Z_{\text{Class-C}} = Z_{\mathrm{A}} \parallel Z_X = \begin{cases} R_L & \omega = 0 \\ Z_X(\omega_0) & \omega = \omega_0 \\ 0 & \omega = 2\omega_0 \\ 0 & \omega = 3\omega_0 \\ 0 & \omega = 4\omega_0 \end{cases} \quad (3)$$

According to equation (3), the proposed Class-C harmonic network provides R_{L} at ω = 0 (DC), which means the structure can provide a DC path during rectifying the power. In addition, it provides $Z_{\mathrm{X}}(\omega_0)$ at fundamental frequency ($\omega = \omega_0$), which can help matching network to compensate the imaginary part of Schottky diode ($Z_{\mathrm{Diode}} = R_{\mathrm{D}}$ - jX_{D}). At $2\omega_0$, $3\omega_0$ and $4\omega_0$,

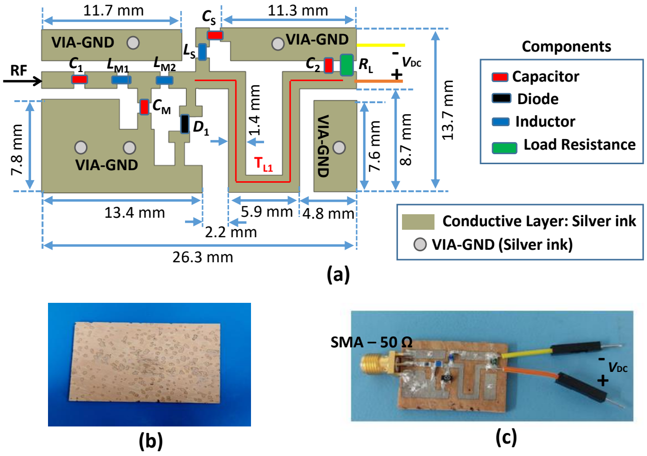

Fig. 4. The proposed Class-C rectifier, (a) Schematic/PCB layout. (b) Cork substrate. (c) fabricated sample. List of Components: Diode: HSMS2820 (package: SOT-23), R_L = 160 Ω (package 1206) SMD resistor from Welwyn, C_1 = 3 pF (Package 0603), C_2 = 100 pF (Package 0603), C_M = 1 pF (Package 0603), C_S = 0.3 pF (Package 0603), $L_{\mathrm{M}1}$ = 3 nH (Package 0805HT), $L_{\mathrm{M}2}$ = 6.8 nH (Package 0805HP), L_S = 1.15 nH (Package 0604HQ). All capacitors are Multi-layer Ceramic Capacitors MLCC-SMD/SMT from the Murata Electronics, and all indicators are from the Coilcraft.

it generates a short-circuited impedance, which is necessary for reshaping the voltage and current waveforms of the diode and fulfilling the Class-C harmonic termination conditions. A Class-C rectifier can be realized by selecting suitable values for the lumped components in the series filter and determining an appropriate characteristic impedance for TL_1.

B. Rectifier Design

A Schottky diode (HSMS-2820-BLKG) from Broadcom/Avago in a shunt topology is employed as the RF-to-DC element. A simple T-type matching network using lumped components is designed to match input impedance of rectifier (Z_IN showed in Fig. 3) to a 50 Ω standard impedance of Signal generator. The proposed rectifier was fabricated using Screen-Printed technologies in cutting-edge laboratories at Tyndall National Institute, Ireland. A photo of printed circuit board (PCB) layout and fabricated prototype of the proposed rectifier are illustrated in Fig. 4. The final rectifier size is 26.3 mm × 13.7 mm, indicating a compact design. In this paper, the shape of the final rectifier layout was cut on vinyl stencil material using a Cricut machine. The stencil was then placed on the cork substrate, and the cut-out areas were manually filled with silver ink. After the fabricated sample was placed in an oven for drying, the vinyl stencil was removed post-curing. To assemble the components on the PCB, conductive Silver paste (CW2400, a conductive epoxy consisting of a 50% mix of part A and 50% part B) was utilized. To ensure strong adhesion of the components on the PCB, the assembled circuit was subsequently placed in an oven at 50 °C (Centigerad degree) for 5 minutes (for future work, the curing process and temperature should be optimised). In the following section, the performance of the fabricated prototype will be evaluated and discussed.

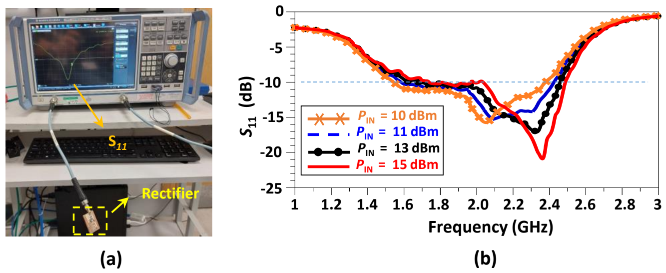

Fig. 5. (a) Experimental setup for measuring S_{11} parameter.(b) Measured S_{11} response for the proposed rectifier at varying P_IN levels. Equipment: Network analyzer: ROHDE & SCHWARZ ZNB 8 Vector Network Analyzer 9KHz to 8.5 GHz.

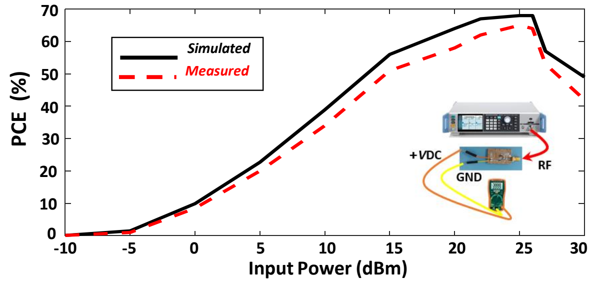

Fig. 6. (a) Simulate and measured PCE results for the proposed rectifier at varying P_IN levels. Equipment: RF signal generator: ROHDE & SCHWARZ SMA-100B up to 6GHz, DC volt-meter: Extech EX330 from EXTECH Instruments.

III. Discussion of Rectifier Performance and Results

This section aims to provide an in-depth discussion of the simulated and measured results for the proposed rectifier. The analysis was carried out in two phases: Phase #1 focuses on a technical discussion of the rectifier's performance, while Phase #2 discusses powering a DC-DC booster and a supercapacitor.

A. Phase #1: Rectifier Performance Evaluation

For evaluation of a rectifier, the reflection coefficient (S_{11}) and PCE are important paramaters to consider. Fig. 5 shows a photo of experimental setup and the measured S_{11} response at different P_IN levels. As shown in Fig. 5(a), the rectifier prototype is connected to a Vector Network Analyser (VNA) to measure S_{11} parameter. Fig. 6 shows the simulated and measured results for the proposed rectifier. According to measurement setup, an RF signal generator was connected to the proposed Class-C rectifier, and a DC volt meter was employed to measure $V_{\mathrm{OUT-DC}}$ across R_L. The resulting PCE was then calculated as:

$$PCE = \frac{P_{\text{OUT-DC}}}{P_{\text{IN}}} = \frac{(V_{\text{OUT-DC}})^2}{R_L} \times \frac{1}{P_{\text{IN}}} \times 100\% \qquad (4)$$

In this equation, $V_{\mathrm{OUT-DC}}$ is the DC voltage at the output of the rectifier, R_L is the output load resistance and P_IN is the RF input power. According to the obtained results shown in Fig. 6, the proposed rectifier has a maximum measured PCE of 64% at P_IN = 24 dBm for an optimum R_L = 160 Ω. According to the obtained results, the proposed Class-C rectifier illustrates a good performance regarding size, PCE

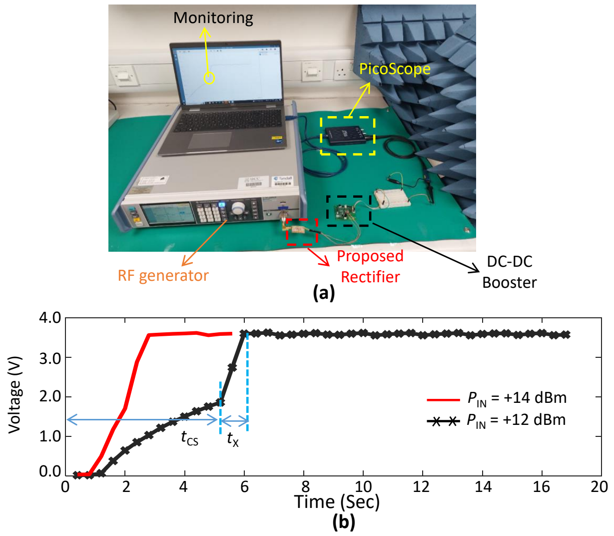

Fig. 7. (a) Experimental setup for powering a DC-DC booster. (b) Measured results of the DC voltage at the booster's output (V_{BAT} pin). Equipment: RF signal generator: ROHDE & SCHWARZ SMA-100B up to 6GHz, DC-DC booster: ADP5090 evaluation board from Analog Devices (ADI), PicoScope: PICOSCOPE 2204A from Pico Technology Ltd.

and S_{11} response, which is required for use in RF energy harvesting and wireless power charging systems.

B. Phase #2: Demonstrating of Powering of an Electronic Circuit

To assess the performance of the rectifier and demonstrate the feasibility of powering an electronic circuit, a DC-DC booster and a supercapacitor are used in the power management setup. The DC-DC booster is employed to supply a sufficient DC voltage, typically 3.3 V, necessary for powering standard electronic circuits and IoT sensors. The ADP5090 evaluation board from Analog Devices (ADI) is selected as a DC-DC boost converter due to its reliable features and operation. Fig. 7 depicts a photo of experimental setup and measured results for powering the ADP5090 booster for varying P_{IN} levels. Figure 7(a) illustrates the experimental setup for powering the DC-DC booster, where a PicoScope used to measure and display the DC voltage at the booster's output (V_{BAT}) denoted on the ADP5090 evaluation board). Fig. 7(b) shows measured V_{BAT} varying P_{IN}levels. The DC-DC boost converter operates in three distinct modes, which are described below.

- Mode 1: The DC-DC booster requires an initial cold-start time (t_{CS}) to increase from 0 V to $V_{\mathrm{Cold-Start}}$ = 1.8 V.
- Mode 2: After reaching this voltage, it switches to fast charging mode, continuing to rise from $V_{\mathrm{Cold-Start}}$ to V_{MAX} = 3.6 V, as represented by t_{X} in Figure 7(b).
- Mode 3: Once V_{MAX} is reached, the system enters a stable mode, delivering a steady DC voltage suitable for powering electronic circuits and IoT devices.

According to obtained results in Fig. 7(b), by increasing P_{IN} level, the DC-DC booster needs a shorter time (t_{CS}) to reach $V_{\mathrm{Cold-Start}}$. In the latter, a supercapacitor (C_{OUT} = 0.33 F) is employed to store the delivered DC power from DC-DC booster and proposed rectifier. Fig. 8 illustrates required

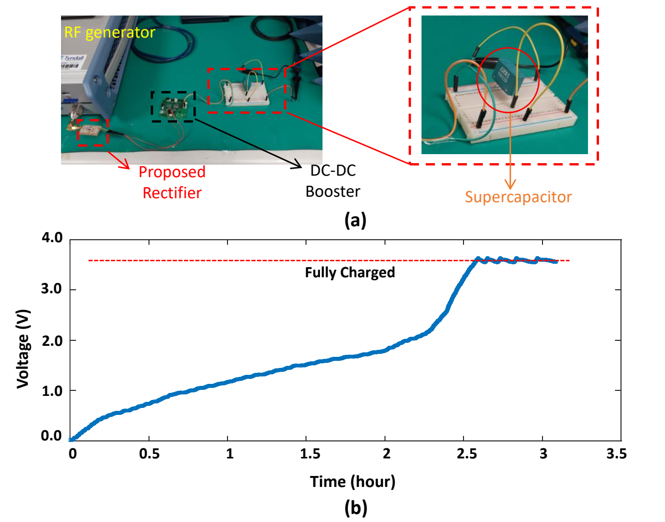

Fig. 8. (a) Experimental setup for charging a supercapacitor (C_{OUT} = 0.33 F). (b) Measured results of the DC voltage across C_{OUT}. at RF P_{IN} level of +12 dBm.

charging time for the supercapacitor for an RF P_{IN} level of 12 dBm. According to Fig. 8 (b), the C_{OUT} = 0.33 F requires 150 minutes time (2.5 hours) to fullycharge the supercapacitor for an RF P_{IN} level of 12 dBm. It is clear that as the P_{IN} level increases, the charging time decreases, and the opposite is true when the P_{IN} level decreases. The proposed system has shown promising performance in powering both the DC-DC booster and a supercapacitor, making it well-suited for powering IoT devices and supporting wireless charging systems.

IV. Conclusions

This paper presented a sustainable and efficient Class-C rectifier for RF energy harvesting and wireless power transmission, fabricated using environmentally friendly materials, a cork substrate and silver nanoparticle ink. The rectifier, designed to operate at 2.4 GHz, achieves a peak PCE of 68%, demonstrating excellent performance at a P_{IN} level of 24 dBm and a load resistance of 160 Ω. The successful integration of a DC-DC boost converter and supercapacitor further validates the rectifier's capability to power IoT devices, showcasing its potential for future applications in sustainable wireless power systems. The use of Cork substrate in designing a microwave Class-C rectifier, a first in this field, opens new possibilities for eco-friendly IoT designs and energy-efficient technologies.

Acknowledgment

This publication has emanated from research conducted with the financial support of Taighde Éireann – Research Ireland and the Department of Agriculture, Food and Marine as well as Enterprise Ireland on behalf of the Government of Ireland under Grant Numbers: SFI 16/RC/3835-2 the SFI Centre VistaMilk; 13/RC/2077 the CONNECT Centre for Future Networks and Communications; SFI/12/RC/2289-2 the Insight Centre for Data Analytics; Grant 16/RC/3918-CONFIRM, and HOLISTICS - Grant EIDT20180291-A. Aspects of this work have also been funded by the EU funded Aurora Project HORIZON-CL2-2022-HERITAGE-01 - 101094245. All work is co-funded under the European Regional Development Fund. For the purpose of Open Access, the author has applied a CC BY public copyright licence to any Author Accepted Manuscript version arising from this submission.

REFERENCES

[1] G. Moloudian, M. Hosseinifard, S. Kumar, R. B. V. B. Simorangkir, J. L. Buckley, C. Song, G. Fantoni, and B. O'Flynn, "Rf energy harvesting techniques for battery-less wireless sensing, industry 4.0, and internet of things: A review," *IEEE Sensors Journal*, vol. 24, no. 5, pp. 5732–5745, 2024.

[2] C. Song, Y. Ding, A. Eid, J. G. D. Hester, X. He, R. Bahr, A. Georgiadis, G. Goussetis, and M. M. Tentzeris, "Advances in wirelessly powered backscatter communications: From antenna/rf circuitry design to printed flexible electronics," *Proceedings of the IEEE*, vol. 110, no. 1, pp. 171–192, 2022.

[3] M. Wagih, A. S. Weddell, and S. Beeby, "Rectennas for radio-frequency energy harvesting and wireless power transfer: A review of antenna design [antenna applications corner]," *IEEE Antennas and Propagation Magazine*, vol. 62, no. 5, pp. 95–107, 2020.

[4] W. A. Khan, R. Raad, F. Tubbal, P. I. Theoharis, and S. Iranmanesh, "Rf energy harvesting using multidirectional rectennas: A review," *IEEE Sensors Journal*, vol. 24, no. 12, pp. 18 762–18 790, 2024.

[5] H. Xiang, Z. Li, H. Liu, T. Chen, H. Zhou, and W. Huang, "Green flexible electronics based on starch," *npj Flexible Electronics*, vol. 6, no. 1, 3 2022. [Online]. Available: http://dx.doi.org/10.1038/s41528-022-00147-x

[6] H. R. et al., "Next-generation iot devices: Sustainable eco-friendly manufacturing, energy harvesting, and wireless connectivity," *IEEE Journal of Microwaves*, vol. 3, no. 1, pp. 237–255, 2023.

[7] T. Tazmeen and F. Q. Mir, "Sustainability through materials: A review of green options in construction," *Results in Surfaces and Interfaces*, vol. 14, p. 100206, 2 2024. [Online]. Available: http://dx.doi.org/10.1016/j.rsurfi.2024.100206

[8] R. Gonçalves, S. Rima, R. Magueta, P. Pinho, A. Collado, A. Georgiadis, J. Hester, N. B. Carvalho, and M. M. Tentzeris, "RFID-based wireless passive sensors utilizing cork materials," *IEEE Sensors Journal*, vol. 15, no. 12, pp. 7242–7251, 2015.

[9] O. Caytan, S. Lemey, S. Agneessens, D. Vande Ginste, P. Demeester, C. Loss, R. Salvado, and H. Rogier, "Half-mode substrate-integrated-waveguide cavity-backed slot antenna on cork substrate," *IEEE Antennas and Wireless Propagation Letters*, vol. 15, pp. 162–165, 2016.

[10] W. Zhai, Y. Zhong, M. Xu, X. Wei, L. Cai, and C. Xia, "Transforming wastes into functional materials: natural cork-based physical structural components and polymers," *Green Chemistry*, 2024.

[11] S. Lemey, O. Caytan, D. V. Ginste, P. Demeester, H. Rogier, and M. Bozzi, "SIW cavity-backed slot multi-antenna systems for the next generation iot applications," in *2016 IEEE Topical Conference on Wireless Sensors and Sensor Networks (WiSNet)*, 2016, pp. 75–77.

[12] H. F. Khalili, S. Lemey, O. Caytan, T. Deckmyn, S. Agneessens, D. V. Ginste, and H. Rogier, "Biodegradable dual semicircular patch antenna tile for smart floors," *IEEE Antennas and Wireless Propagation Letters*, vol. 18, no. 2, pp. 368–372, 2019.

[13] O. Caytan, S. Agneessens, S. Lemey, D. Vande Ginste, P. Demeester, and H. Rogier, "Ultra-wideband cork substrate-integrated-waveguide cavity-backed slot antenna," in *2015 International Conference on Electromagnetics in Advanced Applications (ICEAA)*, 2015, pp. 1104–1107.

[14] S. Rima, A. Georgiadis, A. Collado, R. Goncalves, and N. Carvalho, "Passive UHF RFID enabled temperature sensor tag on cork substrate," in *2014 IEEE RFID Technology and Applications Conference (RFID-TA)*, 2014, pp. 82–85.

[15] G. Moloudian, B. O'Flynn, and J. L. Buckley, "A rectenna design with harmonic suppression for rf energy harvesting applications," in *2023 17th European Conference on Antennas and Propagation (EuCAP)*, 2023, pp. 1–5.

[16] S. Bahrami, G. Moloudian, H.-J. Song, and J. L. Buckley, "Reconfigurable uwb circularly polarized slot antenna with three modes of operation and continuous tuning rang," *IEEE Transactions on Antennas and Propagation*, vol. 70, no. 9, pp. 8542–8547, 2022.

[17] G. Moloudian, S. Bahrami, and R. M. Hashmi, "A microstrip lowpass filter with wide tuning range and sharp roll-off response," *IEEE Transactions on Circuits and Systems II: Express Briefs*, vol. 67, no. 12, pp. 2953–2957, 2020.

[18] G. Moloudain, S. Kumar, B. O'Flynn, and J. L. Buckley, "A compact microwave rectifier for wireless power transfer and energy harvesting applications," in *2024 18th European Conference on Antennas and Propagation (EuCAP)*, 2024, pp. 1–4.

[19] C. Liu, H. Lin, Z. He, and Z. Chen, "Compact patch rectennas without impedance matching network for wireless power transmission," *IEEE Transactions on Microwave Theory and Techniques*, vol. 70, no. 5, pp. 2882–2890, 2022.

[20] P. Lu, X.-S. Yang, J.-L. Li, and B.-Z. Wang, "A compact frequency reconfigurable rectenna for 5.2- and 5.8-GHz wireless power transmission," *IEEE Transactions on Power Electronics*, vol. 30, no. 11, pp. 6006–6010, 2015.

[21] N. Mohammadi, G. Moloudian, S. Roshani, S. Roshani, F. Parandin, and A. Lalbakhsh, "A wilkinson power divider with harmonic suppression through low-pass filter for gsm and lte applications," *Nature-Scientific Reports*, vol. 14, no. 1, 1 2024. [Online]. Available: http://dx.doi.org/10.1038/s41598-024-52506-5

[22] M. Chang, Y. Li, J. Han, H. Liu, and L. Li, "A compact polarization insensitive rectenna with harmonic suppression for wireless power transfer," *IEEE Antennas and Wireless Propagation Letters*, pp. 1–5, 2023.

[23] S. D. Joseph, S. S. H. Hsu, A. Alieldin, C. Song, Y. Liu, and Y. Huang, "High-power wire bonded gan rectifier for wireless power transmission," *IEEE Access*, vol. 8, pp. 82 035–82 041, 2020.

[24] S. Rayatzadeh and G. Moloudian, "Design and fabrication of a miniaturized lowpass-bandpass diplexer with wide tuning range and high isolation," *Journal of Electromagnetic Waves and Applications*, vol. 33, no. 14, pp. 1874–1889, 7 2019. [Online]. Available: http://dx.doi.org/10.1080/09205071.2019.1649604

[25] S. Karimi-khorrami and G. Moloudian, "Design and fabrication of a microstrip lowpass filter with wide tuning range as harmonic suppression with application in wilkinson power divider," *Analog Integrated Circuits and Signal Processing*, vol. 107, no. 1, pp. 155–163, 1 2021. [Online]. Available: http://dx.doi.org/10.1007/s10470-020-01752-4

[26] G. Moloudian and S. Bahrami, "Design and fabrication of a continuous tunable microstrip lowpass filter with wide stopband and sharp response," *International Journal of RF and Microwave Computer-Aided Engineering*, vol. 29, no. 8, 4 2019. [Online]. Available: http://dx.doi.org/10.1002/mmce.21759

[27] X. Y. Zhang, Z.-X. Du, and Q. Xue, "High-efficiency broadband rectifier with wide ranges of input power and output load based on branch-line coupler," *IEEE Transactions on Circuits and Systems I: Regular Papers*, vol. 64, no. 3, pp. 731–739, 2017.

[28] D.-A. Nguyen, H. Nam, and C. Seo, "Design of compact class-F high-efficiency shunt-diode rectifier with extended harmonic termination for wireless power transfer," *IEEE Microwave and Wireless Technology Letters*, vol. 33, no. 1, pp. 78–81, 2023.

[29] G. Moloudian, J. L. Buckley, and B. O'Flynn, "A novel rectenna with class-F harmonic structure for wireless power transfer," *IEEE Transactions on Circuits and Systems II: Express Briefs*, pp. 1–5, 2023.

[30] D.-A. Nguyen, G. T. Bui, H. Nam, Y. Kim, and C. Seo, "A 433-MHz compact inverse class-F rectifier for biomedical wireless power transmission," *IEEE Microwave and Wireless Technology Letters*, vol. 33, no. 6, pp. 759–762, 2023.

[31] D. M. Nguyen, N. D. Au, and C. Seo, "A microwave power transmission system using sequential phase ring antenna and inverted class-F rectenna," *IEEE Access*, vol. 9, pp. 134 163–134 173, 2021.

[32] F. Zhao, D. Inserra, G. Wen, J. Li, and Y. Huang, "A high-efficiency inverse class-F microwave rectifier for wireless power transmission," *IEEE Microwave and Wireless Components Letters*, vol. 29, no. 11, pp. 725–728, 2019.

[33] Z. He, H. Lin, and C. Liu, "A novel class-c rectifier with high efficiency for wireless power transmission," *IEEE Microwave and Wireless Components Letters*, vol. 30, no. 12, pp. 1197–1200, 2020.

[34] Z. Dan, Z. He, H. Lin, and C. Liu, "A patch rectenna with an integrated impedance matching network and a harmonic recycling filter," *IEEE Antennas and Wireless Propagation Letters*, vol. 21, no. 10, pp. 2085–2089, 2022.

[35] *Speag dielectric assessment kit: DAK3.5-TL*, (accessed September 9, 2024). [Online]. Available: https://speag.swiss/products/dak/dak-tl-2/.